Heterodimeric Tacrine-Based Acetylcholinesterase Inhibitors: Investigating Ligand−Peripheral Site Interactions

Paul R. Carlier,*,† Ella S.-H. Chow,† Yifan Han,‡ Jing Liu,‡ Jamal El Yazal,§ and Yuan-Ping Pang§

Departments of Chemistry and Biochemistry, Hong Kong University of Science and Technology, Clear Water Bay, Kowloon, Hong Kong, and Mayo Cancer Center, Department of Pharmacology, Mayo Clinic, 200 First Street SW, Rochester, Minnesota 55905

Received May 5, 1999

Dimeric acetylcholinesterase (AChE) inhibitors containing a single 9-amino-1,2,3,4-tetrahydroacridine (tacrine) unit were constructed in an effort to further delineate structural requirements for optimal binding to the AChE peripheral site. Basic amines of differing hydrophobicity were selected as peripheral site ligands, and in each case, improvements in inhibitory potency and selectivity were seen relative to tacrine itself. AChE IC_{50} values of the optimum dimers decrease significantly as the peripheral site ligand was permuted in the series ammonia > dimethylamine > 4-aminopyridine > 4-aminoquinoline > tacrine. Calculated desolvation free energies of the optimum dimers match the trend in IC_{50} values, suggesting the importance of ligand hydrophobicity for effective cation−π interaction with the peripheral site.

Introduction

We have previously reported the synthesis and evaluation of alkylene-linked dimers of tacrine **1**.[1,2] In vitro, heptylene-linked tacrine dimer **2f** is 149-fold more potent and 250-fold more selective for acetylcholinesterase (AChE) inhibition than **1**, as a result of simultaneous binding of the tacrine units to the catalytic and peripheral sites of AChE (Chart 1, Scheme 1).[2] In vivo (rat cortex or whole brain), 30 min after a single oral administration, **2f** is 10-fold more potent for AChE inhibition than **1**. Furthermore, at doses of **2f** and **1** which afford equivalent in vivo AChE inhibition, **2f** exhibits significantly reduced serum butyrylcholinesterase (BChE) inhibition.[3] Dimer **2f** also exhibits 24-fold greater potency than **1** (rat, oral administration) for reversing scopolamine-induced memory impairments in the standard Morris water maze.[4] These results suggest that **2f** would be a promising drug candidate for palliative treatment of senile dementia of the Alzheimer's type (SDAT).[5] Since the binding of **2f** with the AChE peripheral site is responsible for its enhanced inhibition potency, we sought to design molecular probes which would help elucidate the nature of this interaction. To that end, we herein describe the synthesis and cholinesterase inhibition properties of four classes of tacrine heterodimers, which feature systematic modification of the peripheral site ligand.

Design and Synthesis of Tacrine Heterodimers

X-ray crystallographic studies of inhibitor-bound *Torpedo* AChE reveal two limiting types of binding interactions at the peripheral site. The decamethonium-AChE structure shows stacking of the terminal quaternary group of decamethonium against Trp^{279} in a putative cation−π interaction.[6] Interestingly, uncharged hydrophobic residues can also have affinity for the peripheral site. The recent E2020-AChE structure indicates that the indanone portion of E2020 is stacked against Trp^{279}.[7] A related inhibitor which replaces the indanone moiety of E2020 with a benzisoxazole[8] may also enjoy a similar binding mode. Evidence for the affinity of uncharged hydrophobic residues for the AChE peripheral site was also provided by a study of toluene-tacrine heterodimers **3b**−**h** (Scheme 1).[1] Optimum heterodimer **3f** was only modestly (2.8-fold) more potent than **1**, but the tether length dependence of the potency enhancement was indicative of binding to the peripheral site. Therefore, to elucidate the structural determinants of binding of **2f** at the peripheral site, we designed a series of new heterodimers which feature stepwise mutation of one inhibitor unit from tacrine to a simple amino group. Such heterodimers will be useful for assessing the complementary roles that cation−π and hydrophobic interactions have on peripheral site affinity. It is worth

Chart 1. Tacrine **1** and Dimers **2**[a]

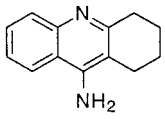

1

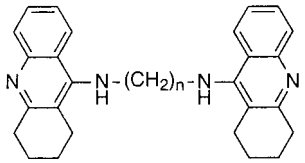

2a-i

[a] Compound lettering system for chart and schemes: **a**, $n = 2$; **b**, $n = 3$; **c**, $n = 4$; **d**, $n = 5$; **e**, $n = 6$; **f**, $n = 7$; **g**, $n = 8$; **h**, $n = 9$; **i**, $n = 10$; **k**, $n = 12$.

* To whom correspondence should be directed: Prof. Paul R. Carlier. Fax: (852) 2358-1594. E-mail: chpaul@ust.hk.
† Department of Chemistry.
‡ Department of Biochemistry.
§ Mayo Cancer Center.

10.1021/jm990224w CCC: $18.00
Published on Web 09/23/1999

Scheme 1. Toluene-Tacrine Heterodimers **3** and Cartoon of Limiting Binding Modes of Heterodimers X-Tacrine to AChE

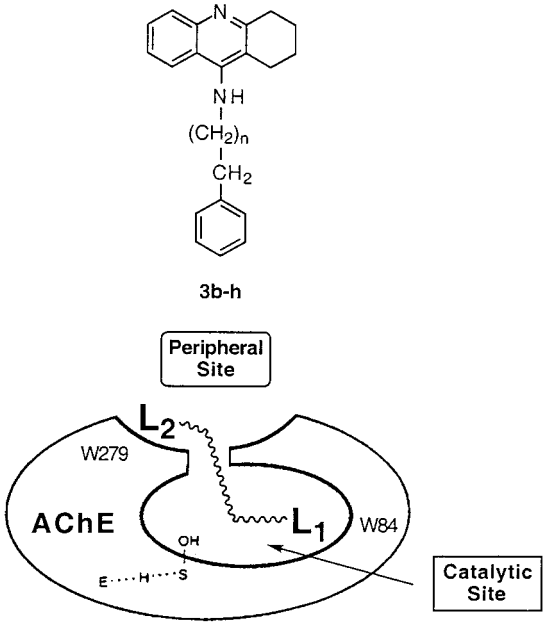

Mode I: L_1 = tacrine, L_2 = X

Mode II: L_1 = X, L_2 = tacrine

noting that such heterodimers might also be useful molecular probes in other systems: similar homodimeric drugs have previously been evaluated as K^+ channel[9] and NMDA receptor[10,11] blockers.

The desired heterodimeric inhibitors were synthesized by modification of the route we have disclosed previously for the synthesis of tacrine dimers **2** (Scheme 2).[2] Combination of 9-chloro-1,2,3,4-tetrahydroacridine (**4**) with 3 equiv of the desired α,ω-diamine in refluxing 1-pentanol provided amino-tacrine heterodimers **5** in good yield (69−91%, Table 1). Subsequent Eschweiler−Clark methylation provided dimethylaminotacrine heterodimers **6** in excellent yield (91−97%, Table 1). Treatment of **5** with 2 equiv of 4-bromopyridine in refluxing 1-pentanol provided 4-aminopyridine-tacrine heterodimers **7**. The low yield of these heterodimers (13−19%, Table 1) was traced to competing reaction of 4-bromopyridine with the solvent, yielding 4-*n*-pentyloxypyridine. Reaction of **5** with 4-chloroquinoline gave 4-aminoquinoline-tacrine heterodimers **8** in moderate yield (36−54%, Table 1). The heterodimer free bases were converted to the corresponding HCl salts by treatment with HCl(g) in $CHCl_3$ and removal of the solvent in vacuo. Elemental analysis (CHN) matched the formulas shown in Table 1 within 0.4% in each case. Assays for rat AChE and BChE inhibition potency were carried out by the Ellman method[12] with some minor modifications, as described previously.[2] Tacrine monomer **1** and dimer **2f** were used as controls, and their cholinesterase IC_{50} values were within error of the previous determination.

Cholinesterase Inhibition

Review of the data in Table 1 reveals that all four heterodimer series show tether length-dependent AChE inhibition potency and selectivity enhancements relative to tacrine **1**, indicating dual-site binding to AChE. In contrast, the heterodimers are uniformly less potent than **1** at BChE, consistent with the absence of a peripheral site on this enzyme.[1] Returning to AChE inhibition, in the aminotacrine heterodimers **5**, optimal potency is provided by an 8-methylene tether (**5g**). In the dimethylaminotacrine heterodimers **6**, tethers of 7 (**6f**), 8 (**6g**), and 10 (**6i**) methylenes provide nearly identical AChE IC_{50} values that are significantly lower than that of tacrine. In the 4-aminopyridine- and 4-aminoquinoline-tacrine heterodimers series **7** and **8**, tether lengths of 7 or 8 methylenes afford the highest AChE potency (12.8−13.6 and 8.8−10.1 nM, respectively). Thus within experimental error, a tether length of 7 or 8 methylenes in all cases provides the optimum AChE affinity. This slight variation is likely due to different optimum binding orientations of the peripheral site ligands and the inability to exactly realize the ideal spacing between the peripheral and catalytic sites with an alkylene chain (the so-called "discontinuity problem"). All of these peripheral site ligands will be protonated under assay conditions and thus can potentially undergo cation−π interaction with Trp^{279}. N−N distance calculations on the fully extended conformations of these optimum dimers reveal that in each case

Scheme 2. Syntheses of Tacrine Heterodimers[a]

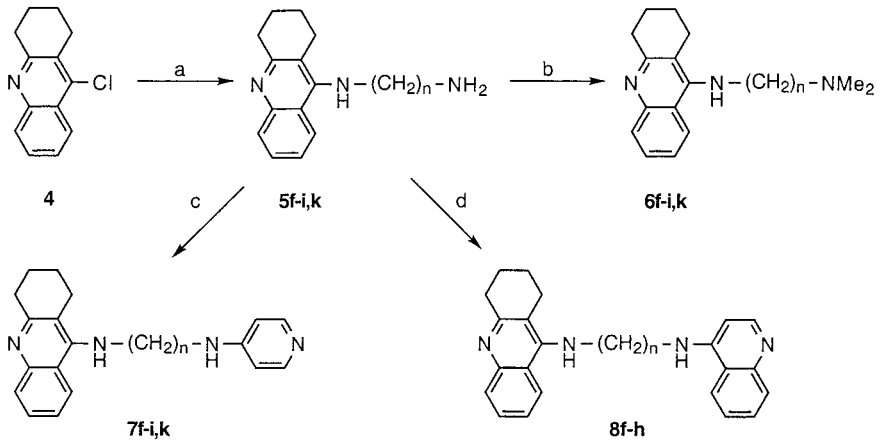

[a] (a) 3.0 equiv $H_2N(CH_2)_nNH_2$, 1-pentanol, 160 °C, 18 h; (b) HCO_2H, HCHO (aq), reflux; (c) 2.0 equiv 4-bromopyridine•HCl, 1-pentanol, 160 °C, 40 h; (d) 2.0 equiv 4-chloroquinoline, 1-pentanol, 160 °C, 40 h.

Table 1. Yields and Cholinesterase Inhibition Constants of Heterodimers and Controls

compd	yield (%)[a]	formula of salt[b]	rat brain AChE IC_{50} (nM)[c]	rat serum BChE IC_{50} (nM)[d]	selectivity for AChE[e]
1	na	$C_{13}H_{14}N_2$•HCl•H_2O	223 ± 11[f]	92 ± 2[f]	0.4
5f	71	$C_{20}H_{29}N_3$•2HCl•H_2O	319 ± 13	357 ± 6	1.1
5g	76	$C_{21}H_{31}N_3$•2HCl•0.8H_2O	89.4 ± 6.2	202 ± 10	2.3
5h	91	$C_{22}H_{33}N_3$•2HCl•1.5H_2O	131 ± 8	687 ± 68	5.2
5i	82	$C_{23}H_{35}N_3$•2HCl•1.5H_2O	147 ± 26	682 ± 82	4.6
5k	69	$C_{25}H_{39}N_3$•2HCl•2H_2O	180 ± 19	791 ± 66	4.4
6f	93	$C_{22}H_{33}N_3$•3HCl•1.1H_2O[g]	52 ± 4	143 ± 7	2.7
6g	91	$C_{23}H_{35}N_3$•1.9HCl•2.5H_2O[g]	47 ± 1	170 ± 1	3.6
6h	97	$C_{24}H_{37}N_3$•2.1HCl•1.4H_2O[g]	71 ± 3	237 ± 17	3.4
6i	95	$C_{25}H_{39}N_3$•2.2HCl•1.1H_2O[g]	45 ± 1	581 ± 22	13
6k	91	$C_{27}H_{43}N_3$•2HCl•1.1H_2O	264 ± 1	695 ± 36	2.6
7f	16	$C_{25}H_{32}N_4$•2HCl•2.5H_2O	12.8 ± 4.0	302 ± 28	24
7g	13	$C_{26}H_{34}N_4$•2HCl•3H_2O	13.6 ± 3.9	157 ± 9	12
7h	19	$C_{27}H_{36}N_4$•2HCl•3H_2O	83.6 ± 8.8	200 ± 11	2.4
7i	19	$C_{28}H_{38}N_4$•2HCl•1.3H_2O	176 ± 26	427 ± 44	2.4
7k	14	$C_{30}H_{42}N_4$•2HCl•2H_2O	261 ± 16	377 ± 30	1.4
8f	36	$C_{29}H_{34}N_4$•2HCl•2.5H_2O	10.1 ± 1.4	110 ± 4	11
8g	52	$C_{30}H_{36}N_4$•3.4HCl•1.7H_2O[g]	8.8 ± 1.3	126 ± 17	14
8h	54	$C_{31}H_{38}N_4$•2HCl•3H_2O	38.7 ± 5.7	156 ± 13	4.0
2f	na	$C_{33}H_{42}N_4$•2HCl•2H_2O	1.5 ± 0.3[f]	149 ± 23[f]	99.4
2g	na	$C_{34}H_{44}N_4$•2HCl•2H_2O	7.8 ± 0.9[f]	105 ± 13[f]	13.5

[a] Yield of free base after chromatography. Compound 1 (tacrine) was purchased from Sigma; dimers **2f**,**g** were prepared according to ref 2. [b] Formulas provided match the elemental analysis within 0.4% (CHN). [c] Assay performed using rat cortex homogenate, in the presence of ethopropazine as a specific BChE inhibitor. [d] Assay performed using rat serum, in the presence of BW284c51 as a specific AChE inhibitor. [e] Selectivity for AChE is defined as IC_{50}(BChE)/IC_{50}(AChE). [f] Data from ref 2. [g] Formula further supported by %Cl analysis.

Table 2. AChE Inhibition Potencies of Selected Drugs Relative to Tacrine **1**

drug	tether length (*n*)	peripheral site ligand X	AChE IC_{50}[a] (nM)	relative potency
1	na	na	223 ± 11	1.0
5g	8	NH_2	89.4 ± 6.2	2.5
6g	8	NMe_2	47.0 ± 1.0	4.7
7f	7	4-aminopyridine	12.8 ± 4.0	17
8f	7	4-aminoquinoline	10.1 ± 1.4	22
2f	7	tacrine	1.5 ± 0.3	149
4-aminoquinoline	na	na	50700 ± 5350	0.004
4-aminopyridine	na	na	>500000	<0.0004

[a] Except for 4-aminoquinoline and 4-aminopyridine, IC_{50} values are taken from Table 1.

it is possible to span the 12 Å distance seen between quaternary groups in the decamethonium-AChE structure.[6]

The most potent heterodimers **8f,g** achieve affinity in the 10 nM range but are less potent than tacrine homodimer **2f** (IC_{50} = 1.5 ± 0.3 nM). Nevertheless, the data obtained in this study is of value to the extent that it relates heterodimer affinity to binding preferences at the AChE peripheral site. Before beginning such a discussion however, it must be noted that a heterodimeric AChE inhibitor X-tacrine could exhibit two limiting binding modes, as depicted in Scheme 1. We propose that heterodimers **5**−**8** bind predominantly via mode I, for the following reasons. It is well-known that AChE inhibitors have much greater affinity for the catalytic site than the peripheral site, except when the inhibitor is too large to penetrate the active site cleft (e.g. propidium,[13] fasciculin[14]). Therefore, if the affinity of tacrine is much greater than X, mode I will dominate, since it places the potent monomer at the catalytic site. This assumption was made in the analysis of toluene-tacrine heterodimers **3** (Scheme 1), because toluene is not an effective AChE inhibitor. In the present case we make a similar argument, because 4-aminopyridine and 4-aminoquinoline are much weaker AChE inhibitors than tacrine (Table 2) and simple *n*-alkylamines are not effective AChE inhibitors.

Taking this approach, one can review the potencies of the optimum heterodimers as a function of the peripheral site ligand X (Table 2). It is interesting to note that appendage of a simple amino group to tacrine provided only a modest potency enhancement (**5g**, 2.5-fold), similar to the previously reported effect of appending a toluene group (**3f**, 2.8-fold potency enhancement[1]). Conversion of the amino group to a dimethylamino group results in a slightly larger (**6g**, 4.7-fold) potency increase, but still remarkably less than the potency increase enjoyed by tacrine homodimer **2f** (149-fold increase). The increase of potency in the series **5g** (89.4 nM), **6g** (47.0 nM), **7f** (12.8 nM), **8f** (10.1 nM), and finally **2f** (1.5 nM) demonstrates that increasing structural similarity of the peripheral site ligand to tacrine improves affinity for AChE. The same trend in IC_{50} values is also observed if comparisons are made at a fixed tether length of 7 methylenes (**5f** > **6f** > **7f** > **8f** > **2f**) or 8 methylenes (**5g** > **6g** > **7g** > **8g** > **2g**) (see Table 1).

Structural variation of the X unit in heterodimers X-tacrine should affect the strength of the cation−π interaction at the peripheral site. For example, it is known that the interaction of ammonium ion with benzene in the gas phase weakens with increasing methyl substitution: NH_4^+ > $MeNH_3^+$ > Me_3NH^+ > Me_4N^+.[15,16] The observation that the dimethylamino-tacrine heterodimer **6g** is more potent than amino-tacrine heterodimer **5g** therefore suggests that in the

Table 3. Experimental and Calculated Desolvation Free Energies[a]

		desolvation free energy (kcal/mol)			
entry	ligand	exptl	HF/6-31G*//HF/6-31G* CPCM	SM5.4 PDP-PM3	SM5.4 PDA-AM1
1	NH_4^+	79[b]	80	85	85
2	$CH_3NH_3^+$	70[b]	70	74	71
3	$Me_2NH_2^+$	63[b]	65	64	61
4	Me_3NH^+	59[b]	58	57	55
5	4-aminopyridine•H^+	na	55	54	52
6	4-aminoquinoline•H^+	na	51	50	47
7	**1**•H^+	na	48	43	41
8	toluene	0.9[b] 3.18[c]	1	1	1
9	**5g**•$2H^+$	na	nd	133	129
10	**6g**•$2H^+$	na	nd	117	114
11	**7f**•$2H^+$	na	nd	113	108
12	**8f**•$2H^+$	na	nd	107	102
13	**2f**•$2H^+$	na	nd	105	98
14	**3f**•H^+	na	nd	41	36

[a] Desolvation free energies were calculated with the HF/6-31G*//HF/6-31G* method using the CPCM model[18] implemented in GAUSSIAN98[19] and with the AMSOL 6.1 package,[20] using both PM3 and AM1 semiempirical optimization methods. The solvent used in the ab initio and semiempirical calculations was water at 298 K, with dielectric constant $\epsilon = 78.4$. [b] Data from ref 21. [c] Data from ref 22.

series **5g**, **6g**, **7f**, **8f**, and **2f**, another factor overwhelms differences in intrinsic cation−π binding ability. Based on the E2020-AChE structure,[7] it is possible that aromatic stacking interactions at the peripheral site contribute to the high affinities of **7f**, **8f**, and **2f**, relative to **5g** and **6g**. However, we propose that the dominant factor in this series is increasing hydrophobicity of the peripheral site ligand, which improves affinity by decreasing the "desolvation penalty" the dimer must pay upon entering the hydrophobic active site cleft of AChE. Aqueous solvation competes against cation−π interaction, as Dougherty has demonstrated for binding of ammonium and quaternary ammonium guests to ethenoanthracene hosts in water.[17] In his model system, protonated amines typically bind very weakly, because their substantial desolvation penalty overwhelms the enthalpic benefit of cation−π interaction. However, as the amine becomes more hydrophobic (through quaternization), the desolvation penalty is reduced and cation−π interaction provides impressive affinities for the ethenoanthracene host.

To test the hypothesis that hydrophobicity of the peripheral site ligand is a significant determinant of affinity in the series **5g**, **6g**, **7f**, **8f**, and **2f**, desolvation free energies were calculated at the ab initio (HF/6-31G*//HF/6-31-G* method using the CPCM model[18] implemented in GAUSSIAN98[19] and semiempirical levels (AMSOL6.1 package[20] with both PM3 and AM1 optimization) (Table 3). Comparison of calculated desolvation free energies with the available experimental data for ammonium ion,[21] its methylated congeners,[21] and toluene[21,22] indicates excellent agreement at the ab initio level (Table 3, entries 1−4, 8). Semiempirical calculations also provide reasonable accuracy for these substrates and closely parallel the ab initio data in cases where experimental data are not available (Table 3, entries 5−7). Given the greater convenience and reasonable accuracy of the semiempirical method, this approach was employed to calculate desolvation free energies for the optimum dimers **5g**, **6g**, **7f**, **8f**, and **2f** (Table 3, entries 9−13). As can be seen, there is a steady decrease in desolvation free energy from **5g** to **2f**, using both the PM3 and AM1 optimization methods. This trend in desolvation free energies exactly parallels the trend in IC_{50} (Table 2). It is worth noting that the trend in calculated desolvation free energies for the isolated peripheral site ligands (Table 3, entries 1, 3, 5−7) also parallels the trend in IC_{50} values for the corresponding heterodimers. We stress that it is the trend in desolvation free energies, not the absolute values themselves, that is significant. Based on the decamethonium-Torpedo AChE X-ray structure,[6] several water molecules can be accommodated in the active site cleft and peripheral site of dimeric inhibitor-bound AChE. Therefore it is expected that the actual desolvation penalty for binding of a particular ligand will be somewhat less than its desolvation free energy.

The calculated desolvation free energies may also help to shed light on the near-equal potencies of toluene-tacrine heterodimer **3f** and aminotacrine heterodimer **5g** (2.8- and 2.5-fold more potent than tacrine, respectively). If the desolvation free energies for these two compounds were also similar, one might conclude that an ammonium group and a benzene ring bind to the peripheral site with near-equal intensity. In fact the calculated desolvation free energy of **5g** is much higher than that of **3f** (Table 3, entries 9, 14), which we propose reflects a smaller but still significant difference in desolvation penalty for these two ligands. The similar affinities of **3f** and **5g** for AChE, coupled with the significantly lower desolvation free energy of **3f**, suggest that an ammonium group interacts much more strongly with the aromatic residue-rich peripheral site than does a benzene ring, a conclusion that is consistent with experiment. In the gas phase, the interaction of $MeNH_3^+$ with benzene has been measured to be worth approximately 19 kcal/mol;[16] in contrast, aromatic−aromatic binding interactions (T-shaped or stacked) are calculated to contribute only 2−3 kcal/mol.[23] Thus, we have demonstrated that both cation−π binding ability and hydrophobicity of the peripheral site ligand are important for achieving high affinity of a bivalent AChE inhibitor.

Conclusion

A series of tacrine heterodimers containing amine peripheral site ligands of varying hydrophobicity were prepared. In each case tether length-dependent potency

enhancements were seen relative to tacrine **1**, indicating dual-site binding. IC_{50} values for the optimum heterodimers decrease significantly as the peripheral site ligand is permuted in the series ammonia > dimethylamine > 4-aminopyridine > 4-aminoquinoline > tacrine, matching the trend seen in calculated desolvation free energies. The similar potency of toluene-tacrine heterodimer **3f** and aminotacrine heterodimer **5g** is attributed to a counterbalance of strong peripheral site cation$-\pi$ interaction and unfavorable desolvation thermodynamics in the latter. In summary these results attest to the importance of peripheral site ligand cation$-\pi$ binding ability and hydrophobicity (low desolvation free energy) in the high potency of tacrine homodimer **2f**.

Experimental Section

9-Amino-1,2,3,4-tetrahydroacridine (**1**) was obtained from Sigma as the HCl salt (monohydrate). 9-Chloro-1,2,3,4-tetrahydroacridine was prepared according to the literature method.[2] ^{1}H and ^{13}C NMR spectra were recorded at 300 and 75 MHz, respectively. Chemical ionization (CI) mass spectra were acquired using CH_4 as the reagent gas. Elemental analysis was performed by the Shanghai Institute of Organic Chemistry, Chinese Academy of Sciences (Shanghai, P.R.C.).

***N*-9′-(1′,2′,3′,4′-Tetrahydroacridinyl)-1,7-diaminoheptane Bis-hydrochloride (5f•2HCl).** 9-Chloro-1,2,3,4-tetrahydroacridine (**4**) (1.0 g, 4.61 mmol), 1,7-diaminoheptane (1.80 g, 13.8 mmol), and 1-pentanol (5 mL) were combined and heated to reflux (160 °C) for 18 h. After cooling to room temperature, the mixture was diluted with CH_2Cl_2 (50 mL) and then washed with 10% NaOH (1 × 50 mL) and water (2 × 40 mL). The organic layer was then dried over $MgSO_4$, filtered, concentrated in vacuo, and purified by flash column chromatography (30% MeOH$-CH_2Cl_2$ with 7 mL of concentrated NH_3 per liter) to afford **5f** as an oil (1.02 g, 71%). The bis-HCl salt was prepared by redissolving the oil in chloroform and purging with HCl gas for 2 min, followed by concentration in vacuo to give **5f**•2HCl as a yellow foam. ^{1}H NMR (CD_3OD): δ 1.24−1.47 (m, 8H), 1.52 (apparent 5-let, J = 7.2 Hz, 2H), 1.64 (apparent 5-let, J = 7.2 Hz, 2H), 1.86−1.90 (m, 4H), 2.70−2.78 (m, 6H), 2.93−2.95 (m, 2H), 3.55 (t, J = 7.2 Hz, 2H), 7.34 (ddd, J = 1.1, 7.2, 8.7 Hz, 1H), 7.56 (apparent d, J = 1.4, 6.9, 8.4 Hz, 1H), 7.74 (dd, J = 0.8, 8.7 Hz, 1H), 8.10 (dd, J = 0.8, 8.6 Hz, 1H); ^{13}C NMR (CD_3OD): δ 23.93, 24.42, 26.47, 28.03, 28.23, 30.49, 30.82, 32.59, 33.99, 41.82, 43.29, 116.68, 121.18, 125.19, 125.40, 127.34, 130.82, 147.24, 154.37, 158.52; MS (CI+): calcd 311, found 312 (M + 1). Anal. ($C_{20}H_{29}N_3$•2HCl•$1H_2O$) C, H, N.

***N*-9′-(1′,2′,3′,4′-Tetrahydroacridinyl)-1,8-diaminooctane Bis-hydrochloride (5g•2HCl). 4** (1.0 g, 4.61 mmol) and 1,8-diaminooctane (1.99 g, 13.8 mmol) were combined as above to afford **5g** as an oil (1.26 g, 76%). The bis-HCl salt was prepared as above and was a yellow foam. ^{1}H NMR (CD_3OD): δ 1.31 (s, 8H), 1.55−1.69 (m, 4H), 1.88−1.91 (m, 4H), 2.71 (s, 2H), 2.83 (t, J = 7.6 Hz, 2H), 2.98 (s, 2H), 3.67 (t, J = 7.2 Hz, 2H), 7.42 (ddd, J = 1.4, 7.0, 8.4 Hz, 1H), 7.64 (apparent d, J = 1.3, 6.9, 8.3 Hz, 1H), 7.76 (apparent d, J = 8.6 Hz, 1H), 8.18 (apparent d, J = 8.5 Hz, 1H); ^{13}C NMR (CD_3OD): δ 23.58, 24.23, 26.25, 27.94, 28.25, 29.84, 30.64, 32.49, 32.96, 41.53, 49.82, 80.02, 115.90, 120.32, 125.68, 125.80, 131.83, 145.51, 155.51, 156.96; MS (CI+): calcd 325, found 326 (M + 1). Anal. ($C_{21}H_{31}N_3$•2HCl•$0.8H_2O$) C, H, N.

***N*-9′-(1′,2′,3′,4′-Tetrahydroacridinyl)-1,9-diaminononane Bis-hydrochloride (5h•2HCl). 4** (1.0 g, 4.61 mmol) and 1,9-diaminononane (2.19 g, 13.8 mmol) were combined as above to yield **5h** as an oil (1.46 g, 94%). The bis-HCl salt was prepared as above and was a yellow foam. ^{1}H NMR (CD_3OD): δ 1.34 (s, 10H), 1.61−1.96 (m, 8H), 2.68−2.70 (m, 2H), 2.90 (t, J = 7.7 Hz, 2H), 3.01−3.05 (m, 2H), 3.94 (t, J = 7.3 Hz, 2H), 7.57 (ddd, J = 2.7, 5.7, 8.6 Hz, 1H), 7.80−7.84 (m, 2H), 7.38 (apparent d, J = 8.7 Hz, 1H); ^{13}C NMR (CD_3OD): δ 22.37, 23.51, 25.43, 27.96, 28.16, 29.07, 29.82, 30.61, 30.67, 30.85, 32.03, 41.28, 49.62, 113.36, 117.58, 120.75, 126.82, 126.91, 134.57, 140.30, 152.27, 158.53; MS (CI+): calcd 339, found 340 (M + 1). Anal. ($C_{22}H_{33}N_3$•2HCl•$1.5H_2O$) C, H, N.

***N*-9′-(1′,2′,3′,4′-Tetrahydroacridinyl)-1,10-diaminodecane Bis-hydrochloride (5i•2HCl). 4** (1.0 g, 4.61 mmol) and 1,10-diaminodecane (2.38 g, 13.8 mmol) were combined as above to yield **5i** as an oil (1.34 g, 82%). The bis-HCl salt was prepared as above and was a yellow foam. ^{1}H NMR (CD_3OD): δ 1.33 (s, 12H), 1.59−1.67 (m, 2H), 1.83 (5-let, J = 7.3 Hz, 2H), 1.94−1.97 (m, 4H), 2.67−2.70 (m, 2H), 2.90 (t, J = 7.7 Hz, 2H), 3.0−3.04 (m, 2H), 3.94 (t, J = 7.3 Hz, 2H), 7.57 (ddd, J = 1.8, 6.7, 8.6 Hz, 1H), 7.0.76−7.86 (m, 2H), 7.38 (apparent d, J = 8.6 Hz, 1H); ^{13}C NMR (CD_3OD): δ 22.35, 23.49, 25.42, 27.95, 28.21, 29.05, 29.81, 30.67, 30.77, 30.89, 30.97, 32.03, 41.28, 49.64, 113.32, 117.52, 120.61, 126.81, 127.0, 134.58, 140.25, 152.15, 158.49; MS (CI+): calcd 353, found 354 (M + 1). Anal. ($C_{23}H_{35}N_3$•2HCl•$1.5H_2O$) C, H, N.

***N*-9′-(1′,2′,3′,4′-Tetrahydroacridinyl)-1,12-diaminododecane Bis-hydrochloride (5k•2HCl). 4** (1.0 g, 4.61 mmol) and 1,12-diaminododecane (2.77 g, 13.8 mmol) were combined as above to yield **5k** as an oil (1.23 g, 69%). The bis-HCl salt was prepared as above and was a yellow foam. ^{1}H NMR (CD_3OD): δ 1.3−1.35 (m, 16H), 1.65 (5-let, J = 7.4 Hz, 2H), 1.83 (5-let, J = 7.2 Hz, 2H), 1.91−1.97 (m, 4H), 2.68−2.70 (m, 2H), 2.91 (t, J = 7.6 Hz, 2H), 3.02−3.04 (m, 2H), 3.95 (t, J = 7.3 Hz, 2H), 7.57 (ddd, J = 1.6, 6.8, 8.6 Hz, 1H), 7.77−7.88 (m, 2H), 7.39 (apparent d, J = 8.7 Hz, 1H); ^{13}C NMR (CD_3OD): δ 22.36, 23.49, 25.40, 27.98, 28.22, 29.08, 29.81, 30.74, 30.81, 31.02, 31.12, 32.03, 41.29, 49.65, 113.33, 117.55, 120.62, 126.81, 127.01, 134.59, 140.27, 152.16, 15.52; MS (CI+): calcd 381, found 382 (M + 1). Anal. ($C_{25}H_{39}N_3$•2HCl•$2H_2O$) C, H, N.

***N*,*N*-Dimethyl-*N*′-9′-(1′,2′,3′,4′-tetrahydroacridinyl)-1,7-diaminoheptane, Hydrochloride Salt (6f•3HCl). 5f** (397 mg, 1.28 mmol), formaldehyde (36.5 wt % in H_2O, 388 μL, 5.10 mmol), and formic acid (98%, 390 μL, 10.2 mmol) were refluxed in methanol (2 mL) for 12 h. Removal of methanol in vacuo, addition of 10% NaOH (30 mL), extraction with CH_2Cl_2 (3 × 30 mL), drying ($MgSO_4$), and concentration in vacuo provided **6f** free base as a brown oil (372 mg). Addition of aqueous HCl (3.0 equiv) and concentration in vacuo provided **6f**•2HCl as a yellow foam (487 mg, 93%). ^{1}H NMR (CD_3OD): δ 1.43 (br s, 6H), 1.71−2.01 (m, 8H), 2.69−2.71 (m, 2H), 2.86 (s, 6H), 3.00−3.02 (m, 2H), 3.08−3.13 (m, 2H), 3.96 (t, J = 7.3 Hz, 2H), 7.53−7.61 (m, 1H), 7.76−7.91 (m, 2H), 8.40 (d, J = 8.7 Hz, 1H); ^{13}C NMR (CD_3OD): δ 22.34, 23.49, 25.45, 26.02, 27.80, 27.97, 29.81, 30.22, 31.92, 43.91, 59.43, 113.34, 117.54, 120.60, 126.85, 127.01, 134.57, 140.23, 152.17, 158.47; MS (CI+): calcd 339, found 340.3 (M + 1). Anal. ($C_{22}H_{33}N_3$•3HCl•$1.1H_2O$) C, H, N, Cl.

***N*,*N*-Dimethyl-*N*′-9′-(1′,2′,3′,4′-tetrahydroacridinyl)-1,8-diaminooctane Bis-hydrochloride (6g•2HCl). 5g** (296 mg, 0.91 mmol) was treated as above to afford **6g**•2HCl as a yellow foam (354 mg, 91%). ^{1}H NMR (CD_3OD): δ 1.40 (br s, 8H), 1.71−1.97 (m, 8H), 2.68−2.70 (m, 2H), 2.86 (s, 6H), 3.00−3.03 (m, 2H), 3.07−3.12 (m, 2H), 3.95 (t, J = 7.4 Hz, 2H), 7.58 (ddd, J = 1.6, 7.0, 8.6 Hz, 1H), 7.75−7.87 (m, 2H), 8.39 (d, J = 8.6 Hz, 1H); ^{13}C NMR (CD_3OD): δ 22.34, 23.48, 25.40, 26.10, 27.86, 28.12, 29.80, 30.53, 30.57, 32.01, 43.88, 49.62, 59.49, 113.33, 117.54, 120.59, 126.82, 127.01, 134.60, 140.26, 152.15, 158.49; MS (CI+): calcd 353, found 354.3 (M + 1). Anal. ($C_{23}H_{35}N_3$•1.9HCl•$2.5H_2O$) C, H, N, Cl.

***N*,*N*-Dimethyl-*N*′-9′-(1′,2′,3′,4′-tetrahydroacridinyl)-1,9-diaminononane Bis-hydrochloride (6h•2HCl). 5h** (124 mg, 0.37 mmol) was treated as above to afford **6h**•2HCl as a yellow (156 mg, 97%). ^{1}H NMR (CD_3OD): δ 1.36 (br s, 10H), 1.71−1.95 (m, 8H), 2.62 (s, 2H), 2.86 (s, 6H), 3.02 (s, 2H), 3.10 (t, J = 7.8 Hz, 2H), 3.94 (t, J = 6.9 Hz, 2H), 7.57 (t, J = 7.1 Hz, 1H), 7.77−7.86 (m, 2H), 8.38 (d, J = 8.5 Hz, 1H); ^{13}C NMR (CD_3OD): δ 22.35, 23.50, 25.46, 26.13, 27.93, 28.19, 29.82, 30.57, 30.82, 32.04, 43.94, 49.65, 59.53, 113.31, 117.52, 120.61, 126.83, 127.01, 134.58, 140.23, 152.14, 158.46; MS (CI+): calcd 367, found 368.3 (M + 1). Anal. ($C_{24}H_{37}N_3$•2.1HCl•$1.4H_2O$) C, H, N, Cl.

***N,N*-Dimethyl-*N*′-9′-(1′,2′,3′,4′-tetrahydroacridinyl)-1,-10-diaminodecane Bis-hydrochloride (6i•2HCl). 5i** (563 mg, 1.60 mmol) was treated as above to afford **6i**•2HCl as a yellow foam (688 mg, 95%). ^{1}H NMR (CD_3OD): δ 1.26 (br s, 12H), 1.72−1.97 (m, 8H), 2.68−2.70 (m, 2H), 2.87 (s, 6H), 3.01−3.04 (m, 2H), 3.08−3.13 (m, 2H), 3.94 (t, J = 7.4 Hz, 2H), 7.57 (ddd, J = 1.7, 6.7, 8.6 Hz, 1H), 7.77−7.87 (m, 2H), 8.38 (d, J = 8.7 Hz, 1H); ^{13}C NMR (CD_3OD): δ 22.35, 23.49, 25.41, 26.14, 27.95, 28.20, 29.81, 30.65, 30.76, 30.87, 30.96, 32.02, 43.89, 49.63, 59.51, 113.31, 117.52, 120.60, 126.81, 127.00, 134.58, 140.24, 152.14, 158.47; MS (CI+): calcd 381, found 382.3 (M + 1). Anal. ($C_{25}H_{39}N_3$•2.2HCl•1.1H_2O) C, H, N, Cl.

***N,N*-Dimethyl-*N*′-9′-(1′,2′,3′,4′-tetrahydroacridinyl)-1,-12-diaminododecane Bis-hydrochloride (6k•2HCl). 5k** (363 mg, 0.95 mmol) was treated as above to afford **6k**•2HCl as a yellow foam (418 mg, 91%). ^{1}H NMR (CD_3OD): δ 1.30−1.36 (m, 16H), 1.72−1.97 (m, 8H), 2.70 (s, 2H), 2.87 (s, 6H), 3.02−3.04 (m, 2H), 3.08−3.13 (m, 2H), 3.94 (t, J = 7.3 Hz, 2H), 7.58 (ddd, J = 1.6, 6.9, 8.6 Hz, 1H), 7.76−7.87 (m, 2H), 8.38 (d, J = 8.6 Hz, 1H); ^{13}C NMR (CD_3OD): δ 22.35, 23.49, 25.40, 26.16, 27.98, 28.21, 29.81, 30.71, 30.80, 31.01, 31.10, 32.02, 43.89, 49.65, 59.54, 113.32, 117.54, 120.60, 126.81, 127.01, 134.60, 140.27, 152.14, 158.51; MS (CI+): calcd 409, found 410.3 (M + 1). Anal. ($C_{27}H_{43}N_3$•2HCl•1.1H_2O) C, H, N, Cl.

***N*-4′-Pyridyl-*N*′-9″-(1″,2″,3″,4″-tetrahydroacridinyl)-1,7-diaminoheptane Bis-hydrochloride (7f•2HCl). 5f** (492 mg, 1.58 mmol) and 4-bromopyridine hydrochloride (462 mg, 2.37 mmol) were combined in 1-pentanol (3 mL) and heated to reflux (oil bath temperature 160 °C) for 40 h. After cooling to room temperature, the mixture was diluted with CH_2Cl_2 (50 mL) and washed with 10% NaOH (1 × 50 mL) and water (2 × 40 mL). The organic layer was then dried ($MgSO_4$), filtered, concentrated in vacuo, and purified by flash column chromatography (10% MeOH−CH_2Cl_2 with 7 mL of concentrated NH_3 per liter) to afford **7f** as an oil (116 mg, 16%). Treatment with HCl gas provided **7f**•2HCl. ^{1}H NMR (CD_3OD): δ 1.40 (s, 6H), 1.6−1.97 (m, 8H), 2.60−2.66 (m, 2H), 2.96−2.99 (m, 2H), 2.24−3.30 (m, 2H), 3.91 (t, J = 7.3 Hz, 2H), 6.82 (d, J = 7.4 Hz, 2H), 7.53 (ddd, J = 1.5, 6.9, 8.5 Hz, 1H), 7.72−7.77 (m, 2H), 7.91 (apparent d, J = 6.5 Hz, 1H), 8.05 (apparent d, J = 6.5 Hz, 1H), 8.35 (d, J = 8.6 Hz, 1H); ^{13}C NMR (CD_3OD): δ 22.35, 23.49, 25.42, 28.16, 28.32, 29.81, 30.48, 31.99, 44.34, 49.61, 106.38, 111.74, 113.34, 117.55, 120.61, 126.84, 127.02, 134.60, 139.70, 140.27, 142.11, 152.18, 158.50; MS (CI+): calcd 388, found 389 (M + 1). Anal. ($C_{25}H_{32}N_4$•2HCl•2.5H_2O) C, H, N.

***N*-4′-Pyridyl-*N*′-9″-(1″,2″,3″,4″-tetrahydroacridinyl)-1,8-diaminooctane Bis-hydrochloride (7g•2HCl). 5g** (466 mg, 1.43 mmol) and 4-bromopyridine hydrochloride (697 mg, 3.59 mmol) were combined as above to afford **7g** as an oil (89.8 mg, 13%). Treatment with HCl gas provided **7g**•2HCl. ^{1}H NMR (CD_3OD): δ 1.40 (s, 8H), 1.64−1.97 (m, 8H), 2.67−2.70 (m, 2H), 2.99−3.03 (m, 2H), 2.28−3.34 (m, 2H), 3.95 (t, J = 7.3 Hz, 2H), 6.86 (apparent d, J = 7.5 Hz, 2H), 7.57 (ddd, J = 1.6, 6.8, 8.6 Hz, 1H), 7.76−7.87 (m, 2H), 7.95 (apparent d, J = 6.6 Hz, 1H), 8.10 (d, J = 6.7 Hz, 1H), 8.38 (d, J = 8.6 Hz, 1H); ^{13}C NMR (CD_3OD): δ 22.34, 23.48, 25.40, 28.18, 28.36, 29.80, 30.76, 32.02, 44.36, 49.64, 106.36, 111.72, 113.32, 117.53, 120.60, 126.81, 127.01, 134.59, 139.69, 140.27, 142010, 152.15, 158.49; MS (CI+): calcd 402, found 403 (M + 1). Anal. ($C_{26}H_{34}N_4$•2HCl•3H_2O) C, H, N.

***N*-4′-Pyridyl-*N*′-9″-(1″,2″,3″,4″-tetrahydroacridinyl)-1,9-diaminononane Bis-hydrochloride (7h•2HCl). 5h** (212 mg, 0.622 mmol) and 4-bromopyridine hydrochloride (182 mg, 0.932 mmol) were combined as above to afford **7h** as an oil (49.4 mg, 19%). Treatment with HCl gas provided **7h**•2HCl. ^{1}H NMR (CD_3OD): δ 1.36 (s, 10H), 1.61−1.97 (m, 8H), 2.68−2.70 (m, 2H), 2.99−3.03 (m, 2H), 2.26−3.34 (m, 2H), 3.95 (t, J = 7.4 Hz, 2H), 6.86 (d, J = 7.4 Hz, 2H), 7.57 (apparent t, J = 7.7 Hz, 1H), 7.76−7.86 (m, 2H); 7.95 (d, J = 6.3 Hz, 1H), 8.10 (d, J = 6.4 Hz, 1H), 8.38 (d, J = 8.7 Hz, 1H); ^{13}C NMR (CD_3OD): δ 22.35, 23.49, 25.40, 28.22, 28.44, 29.81, 29.91, 30.77, 30.82, 31.03, 32.04, 44.39, 49.65, 106.36, 111.72, 113.33, 117.55, 120.60, 126.81, 127.02, 134.60, 139.70, 140.28, 142.10, 152.15, 158.51; MS (CI+): calcd 416, found 417 (M + 1). Anal. ($C_{27}H_{36}N_4$•2HCl•3H_2O) C, H, N.

***N*-4′-Pyridyl-*N*′-9″-(1″,2″,3″,4″-tetrahydroacridinyl)-1,-10-diaminodecane Bis-hydrochloride (7i•2HCl). 5i** (767 mg, 2.17 mmol) and 4-bromopyridine hydrochloride (442 mg, 2.27 mmol) were combined as above to afford **7i** as an oil (210 mg, 19%). Treatment with HCl gas provided bis-HCl salt **7i**•2HCl. ^{1}H NMR (CD_3OD): δ 1.32 (s, 12H), 1.61−2.01 (m, 8H), 2.69 (s, 2H), 3.01 (s, 2H), 3.28−3.34 (m, 2H), 3.94 (t, J = 7.3 Hz, 2H), 6.87 (d, J = 7.3 Hz, 2H), 7.57 (ddd, J = 1.7, 6.7, 8.6 Hz, 1H), 7.77−7.91 (m, 2H); 7.95 (apparent d, J = 6.4 Hz, 1H), 8.09 (apparent d, J = 7.8 Hz, 1H), 8.38 (d, J = 8.6 Hz, 1H); ^{13}C NMR (CD_3OD): δ 22.35, 23.49, 25.41, 28.20, 28.44, 29.80, 29.90, 30.78, 30.87, 31.04, 32.02, 44.39, 49.64, 106.36, 111.72, 113.31, 117.53, 120.60, 126.80, 127.01, 134.58, 139.67, 140.25, 142.09, 152.14, 158.49; MS (CI+): calcd 430, found 431 (M + 1). Anal. ($C_{28}H_{38}N_4$•2HCl•1.3H_2O) C, H, N, Cl.

***N*-4′-Pyridyl-*N*′-9″-(1″,2″,3″,4″-tetrahydroacridinyl)-1,-12-diaminododecane Bis-hydrochloride (7k•2HCl). 5k** (433 mg, 1.14 mmol) and 4-bromopyridine hydrochloride (333 mg, 1.70 mmol) were combined as above to yield **7k** as an oil (81.5 mg, 14%). Treatment with HCl gas provided **7k**•2HCl. ^{1}H NMR (CD_3OD): δ 1.29−1.41 (m, 16H), 1.82 (5-let, J = 7.3 Hz, 2H), 1.66 (5-let, J = 7.2 Hz, 2H), 1.95−2.01 (m, 4H), 2.68−2.70 (m, 2H), 3.0−3.07 (m, 2H), 3.29−3.34 (m, 2H), 3.95 (t, J = 7.3 Hz, 2H), 6.87 (d, J = 7.5 Hz, 2H), 7.57 (ddd, J = 1.7, 6.8, 8.6 Hz, 1H), 7.76−7.87 (m, 2H), 7.95 (apparent d, J = 6.3 Hz, 1H), 8.10 (apparent d, J = 6.2 Hz, 1H), 8.39 (d, J = 8.6 Hz, 1H); ^{13}C NMR (CD_3OD): δ 22.37, 23.51, 25.42, 28.22, 28.48, 29.82, 29.93, 30.81, 30.93, 31.11, 31.15, 31.18, 32.04, 44.41, 49.67, 106.38, 111.74, 113.34, 117.56, 120.62, 126.83, 127.04, 134.61, 139.90, 140.28, 142.11, 152.16, 158.53; MS (CI+): calcd 458, found 459 (M + 1). Anal. ($C_{30}H_{42}N_4$•2HCl•2H_2O) C, H, N.

***N*-4′-Quinolyl-*N*′-9″-(1″,2″,3″,4″-tetrahydroacridinyl)-1,7-diaminoheptane Bis-hydrochloride (8f•2HCl). 5f** (190 mg, 0.61 mmol) and 4-chloroquinoline (200 mg, 1.22 mmol) were combined as above to yield **8f** as an oil (95.6 mg, 36%). Treatment with HCl gas provided **8f**•2HCl. ^{1}H NMR (CD_3OD): δ 1.47 (s, 6H), 1.78−2.01 (m, 8H), 2.68 (broad s, 2H), 3.00−3.02 (m, 2H), 3.59 (t, J = 7.2 Hz, 2H), 3.94 (t, J = 7.4 Hz, 2H), 6.85 (d, J = 7.1 Hz, 1H), 7.54−7.92 (m, 6H), 8.34−8.43 (m, 3H); ^{13}C NMR (CD_3OD): δ 22.33, 23.48, 25.42, 28.13, 28.39, 29.56, 29.80, 30.48, 31.96, 45.24, 99.67, 113.30, 117.49, 118.77, 120.59, 121.52, 124.43, 126.81, 126.99, 128.60, 134.56, 135.33, 139.70, 140.21, 143.49, 152.12, 158.11, 158.42; HPLC: 25.72 min, 98.6% area; MS (CI+): calcd 438, found 439 (M + 1). Anal. ($C_{29}H_{34}N_4$•2HCl•2.5H_2O) C, H, N.

***N*-4′-Quinolyl-*N*′-9″-(1″,2″,3″,4″-tetrahydroacridinyl)-1,8-diaminooctane, Hydrochloride Salt (8g•3.4HCl). 5g** (213 mg, 0.65 mmol) and 4-chloroquinoline (214 mg, 1.31 mmol) were combined as above to afford **8g** as an oil (155 mg, 52%). Treatment with HCl gas provided **8g**•2HCl. ^{1}H NMR (CD_3OD): δ 1.42 (s, 8H), 1.77−1.96 (m, 8H), 2.67−2.9 (m, 2H), 3.01−3.03 (m, 2H), 3.58 (t, J = 7.3 Hz, 2H), 3.94 (t, J = 7.3 Hz, 2H), 6.85 (d, J = 7.2 Hz, 1H), 7.56−7.90 (m, 6H), 8.35−8.43 (m, 3H); ^{13}C NMR (CD_3OD): δ 22.37, 23.51, 25.44, 28.20, 28.49, 29.66, 29.82, 30.75, 30.81, 32.04, 45.32, 49.65, 99.069, 113.33, 117.53, 118.82, 120.62, 121.56, 124.43, 126.83, 127.04, 128.64, 134.60, 135.37, 139.75, 140.27, 143.51, 152.16, 158.16, 158.49; MS (CI+): calcd 452, found 453 (M + 1). Anal. ($C_{30}H_{36}N_4$•3.4HCl•1.7H_2O) C, H, N, Cl.

***N*-4′-Quinolyl-*N*′-9″-(1″,2″,3″,4″-tetrahydroacridinyl)-1,9-diaminononane, Bis-hydrochloride Salt (8h•2HCl). 5h** (200 mg, 0.59 mmol) and 4-chloroquinoline (193 mg, 1.18 mmol) were combined as above to afford **8h** as an oil (139 mg, 44%). Treatment with HCl gas provided **8h**•2HCl. ^{1}H NMR (CD_3OD): δ 1.37−1.45(m, 10H), 1.74−2.01 (m, 8H), 2.67−2.69 (m, 2H), 2.99−3.03 (m, 2H), 3.58 (t, J = 7.5 Hz, 2H), 3.93 (t, J = 7.3 Hz, 2H), 6.85 (d, J = 7.2 Hz, 1H), 7.54−7.90 (m, 6H), 8.35−8.43 (m, 3H); ^{13}C NMR (CD_3OD): δ 22.35, 23.48, 25.40, 28.20, 28.52, 29.66, 29.80, 30.73, 30.83, 31.00, 32.03, 45.32, 49.64, 99.66, 113.31, 117.52, 118.79, 120.60, 121.54, 124.39, 126.81, 127.00, 128.63, 134.59, 135.35, 139.74, 140.25, 143.49,

152.13, 158.14, 158.48; MS (CI+): calcd 466, found 467 (M + 1). Anal. ($C_{31}H_{38}N_4$•2HCl•3H_2O) C, H, N.

Enzyme Preparation and AChE/BChE Inhibition Studies. AChE and BChE enzyme preparations were prepared from cortex and serum, respectively, of decapitated rats. Frontal cortex (brain dissected on ice) was homogenized in sodium phosphate buffer (39 vol, 75 mM, pH 7.4). Rat serum was obtained by centrifugation of blood (3500*g*, 10 min). The cholinesterase assays were performed using the colorimetric method of Ellman,[12] with minor modification. For determination of AChE inhibition, cortex homogenate was preincubated for 5 min with ethopropazine (0.1 mM), a selective inhibitor of BChE. Similarly, for determination of BChE inhibition, serum was preincubated with BW284c51 (0.01 mM), a selective inhibitor of AChE. A mixture of 4 mL containing acetylthiocholine iodide (0.3 mM) or butrylthiocholine iodide (0.4 mM), 1 mL of sodium phosphate buffer (0.1 mM, pH 7.4), a solution of the compound being tested (0.1 mL), and homogenate or serum (0.1 mL) was incubated at 37 °C for 8 min. The reaction was terminated by the addition of sodium dodecyl sulfate (3% w/v, 1 mL), after which the 5,5′-dithiobis(2-nitrobenzoic acid) indicator (0.2% w/v, 1 mL) was added. Enzyme activity was determined by measuring the absorbance at 420 nm after 10 min, relative to the drug-free control. Triplicate measurements were performed at typically a total of 8 drug concentrations; IC_{50} values were determined from a plot of enzyme activity vs −log [drug].

Acknowledgment. We thank the Research Grants Council of Hong Kong (HKUST6156/97M) and the Biotechnology Research Institute (HKUST) for financial support.

References

(1) Pang, Y.-P.; Quiram, P.; Jelacic, T.; Hong, F.; Brimijoin, S. Highly Potent, Selective, and Low Cost Bis-tetrahydroaminacrine Inhibitors of Acetylcholinesterase. *J. Biol. Chem.* **1996**, *271*, 23646−23649.

(2) Carlier, P. R.; Han, Y. F.; Chow, E. S.-H.; Li, C. P.-L.; Wang, H.; Lieu, T. X.; Wong, H. S.; Pang, Y.-P. Evaluation of Short-Tether Bis-THA AChE Inhibitors. A Further Test of the Dual Binding Site Hypothesis. *Bioorg. Med. Chem.* **1999**, *7*, 351−357.

(3) Wang, H.; Carlier, P. R.; Ho, W. L.; Wu, D. C.; Lee, N. T. K.; Li, C. P. L.; Pang, Y. P.; Han, Y. F. Effects of bis(7)-tacrine, a novel anti-Alzheimer's agent, on rat brain AChE. *NeuroReport* **1999**, *10*, 789−793.

(4) Wang, H.; Carlier, P. R.; Ho, W.-l.; Lee, N. T.-K.; Pang, Y.-P.; Han, Y.-f. Attenuation of scopolamine-induced deficits in navigational performance in rats by bis(7)-tacrine, a novel dimeric AChE inhibitor. *Acta Pharm. Sin.* **1999**, *20*, 211−217.

(5) Albert, E.; Phillip, F. In *Alzheimer Disease*: *From Molecular Biology to Therapy*; Berker, R., Giacoboni, E., Eds.; Birkhauser Press: Boston, 1996; pp 211−215.

(6) Harel, M.; Schalk, I.; Ehret-Sabatier, L.; Bouet, F.; Goeldner, M.; Hirth, C.; Axelsen, P. H.; Silman, I.; Sussman, J. L. Quaternary ligand binding to aromatic residues in the active-site gorge of acetylcholinesterase. *Proc. Natl. Acad. Sci. U.S.A.* **1993**, *90*, 9031−9035.

(7) Kryger, G.; Silman, I.; Sussman, J. L. Structure of acetylcholinesterase complexed with E2020 (Aricept): implications for the design of new anti-Alzheimer drugs. *Structure* **1999**, *7*, 297−307.

(8) Villalobos, A.; Butler, T. W.; Chapin, D. S.; Chen, Y. L.; DeMattos, S. B.; Ives, J. L.; Jones, S. B.; Liston, D. R.; Nagel, A. A.; Nason, D. M.; Nielsen, J. A.; Ramírez, A. D.; Shalaby, I. A.; White, W. F. 5,7-Dihydro-3-[2-[1-(phenylmethyl)-4-piperidinyl]ethyl]-6H-pyrrolo[3,2-f]-1,2-benzisoxazol-6-one: A Potent and Centrally-Selective Inhibitor of Acetylcholinesterase with an Improved Margin of Safety. *J. Med. Chem.* **1995**, *38*, 2802−2808.

(9) Galanakis, D.; Davis, C. A.; Herrero, B. D. R.; Ganellin, C. R.; Dunn, P. M.; Jenkinson, D. H. Synthesis and Structure−Activity Relationships of Dequalinium Analogues as K^+ Channel Blockers. Investigations on the Role of the Charged Heterocycle. *J. Med. Chem.* **1995**, *38*, 595−606.

(10) Nelson, M. E.; Albuquerque, E. X. 9-Aminoacridines Act at a Site Different from that for Mg^{2+} in Blockade of the *N*-Methyl-D-Aspartate Receptor Channel. *Mol. Pharmacol.* **1994**, *46*, 151−160.

(11) Bergeron, R. J.; Weimar, W. R.; Wu, Q.; Feng, Y.; McManis, J. S. Polyamine Analogue Regulation of NMDA MK-801 Binding: A Structure−Activity Study. *J. Med. Chem.* **1996**, *39*, 5257−5266.

(12) Ellman, G. L.; Courtney, K. D.; Andres, V. J.; Featherstone, R. M. A new and rapid colorimetric determination of acetylcholinesterase activity. *Biochem. Pharmacol.* **1961**, *7*, 88−95.

(13) Szegletes, T.; Mallender, W. D.; Rosenberry, T. L. Nonequilibrium Analysis Alters the Mechanistic Interpretation of Inhibition of Acetylcholinesterase by Peripheral Site Ligands. *Biochemistry* **1998**, *37*, 4206−4216.

(14) Harel, M.; Kleywegt, G. J.; Ravelli, R. B. G.; Silman, I.; Sussman, J. L. Crystal Structure of an acetylcholinesterase-fasciculin complex: interaction of a three-fingered toxin from snake venom with its target. *Structure* **1995**, *3*, 1355−1366.

(15) Meot-Ner (Mautner), M.; Deakyne, C. A. Unconventional Ionic Hydrogen Bonds. 1. $CH^{\delta+}$...X. Complexes of Quaternary Ions with n- and π-donors. *J. Am. Chem. Soc.* **1985**, *107*, 469−474.

(16) Deakyne, C. A.; Meot-Ner (Mautner), M. Unconventional Ionic Hydrogen Bonds. 2. NH^+....π. Complexes of Onium Ions with Olefins and Benzene Derivatives. *J. Am. Chem. Soc.* **1985**, *107*, 474−479.

(17) Kearney, P. C.; Mizoue, L. S.; Kumpf, R. A.; Forman, J. E.; McCurdy, A.; Dougherty, D. A. Molecular Recognition in Aqueous Media. New Binding Studies Provide Further Insights into the Cation-π Interaction and Related Phenomena. *J. Am. Chem. Soc.* **1993**, *115*, 9907−9919.

(18) Barone, V.; Cossi, M. Quantum Calculation of Molecular Energies and Energy Gradients in Solution by a Conductor Solvent Model. *J. Phys. Chem. A* **1998**, *102*, 1995−2001.

(19) *Gaussian98*; Gaussian Inc.: Carnegie Office Park, Building 6, Pittsburgh, PA, 1998.

(20) Hawkins, G. D.; Cramer, C. J.; Truhlar, D. G. Parametrized Models of Aqueous Free Energies of Solvation Based on Pairwise Descreening of Solute Atomic Charges from a Dielectric Medium. *J. Phys. Chem.* **1996**, *100*, 19824−19839.

(21) Cramer, C. J.; Truhlar, D. G. General Parametrized SCF Model for Free Energies of Solvation in Aqueous Solution. *J. Am. Chem. Soc.* **1991**, *113*, 8305−8311.

(22) Murray, J. S.; Abu-Awwad, F.; Politzer, P. Prediction of Aqueous Solvation Free-Energies from Properties of Solute Molecular-Surface Electrostatic Potentials. *J. Phys. Chem. A* **1999**, *103*, 1853−1856.

(23) Chipot, C.; Jaffe, R.; Maigret, B.; Pearlman, D. A.; Kollman, P. A. Benzene Dimer: A Good Model for π-π Interactions in Proteins? A Comparison between the Benzene and the Toluene Dimers in the Gas Phase and in an Aqueous Solution. *J. Am. Chem. Soc.* **1996**, *118*, 11217−11224.

JM990224W